

# A Case Study for Development of Comprehensive Seismic Risk Assessment

—PART 1 Mechanism of damage occurrence and damage estimation method—

Hitoshi TANIGUCHI and Kumizi IIDA

総合地震危険度評価法に関する研究

—（その1）災害発生の構想と評価法—

谷口仁士・飯田 汲 事

The mechanism of occurrence of disasters caused by earthquakes and its preventive measures have been investigated by taking the past three large earthquakes occurred around Nagoya city as the objects for case study. The supposed disasters may be breakdown of houses, destruction of man-made grounds or slopes, occurrence of fires and, in the worst case, loss of lives. This investigation is each composed of the part 1 and the part 2.

The present paper, part 1, describes the investigations concerned with the mechanism of occurrence and the estimation method of the earthquake damage on the bases of the past large earthquakes.

## 1. INTRODUCTION

Protection of lives and properties of human beings and preservation of urban systems from earthquakes will be very important social problems, especially in cities with dense populations. Considering the graveness of earthquake damage, we should at first elucidate the mechanism of occurrence of earthquake and the disaster caused by them from many viewpoints. To estimate the degree of damage in each dwelling area, it is necessary to analyze wholly and systematically the various phenomena caused by earthquakes which may bring about direct and indirect damages to us in due consideration of circumstances of the urban area. Probable major factors of the damages are great earthquake activity, seismic response of ground and distribution of house and dangerous materials in the urban area. To estimate the degree of damage by earthquake, it is necessary to elucidate relations among the major factors mentioned above and ground conditions, outbreak and spreading fires, and loss of life. Based on the estimating of earthquake damage, we can clarify which factor will bring critical damage in each area and can find useful suggestions to the earthquake-disaster prevention project of urban area for future.

In this paper, we investigate the mechanism of damage occurrence and estimation method of earthquake damage. The mechanism of damage occurrence is studied the propagation of seismic wave from hypocenter to the urban area and the estimation of direct damages caused by earthquake ground motion such as breakdown of houses and ground breakage, and indirect damages such as outbreak and spreading fires. We proposed the method of seismic risk assessment combining the estimated each damages.

## 2. MECHANISM OF DAMAGE OCCURRENCE

As a general concept, a system shown in Figure 1 is considered to investigate the earthquake damages in an area. Seismic wave which generated from an earthquake fault propagates in seismic basement. Seismic wave in the basement is considerably influenced by an amplification in a soil deposit and arrives at the ground surface. Figure 1 is a simplified system of damage occurrence. The seismic wave at the ground surface acts as an impact to regional circumstances. Response characteristics of the seismic impact are from damage 1 to damage m corresponding to variety of earthquake damages as shown in Figure 1. Consequently, the impact to social circumstance at present gives rise to the production of earthquake damage 1.

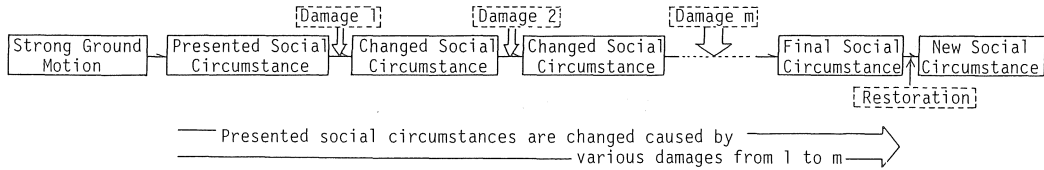


Figure 1 Simplified system of damage occurrence

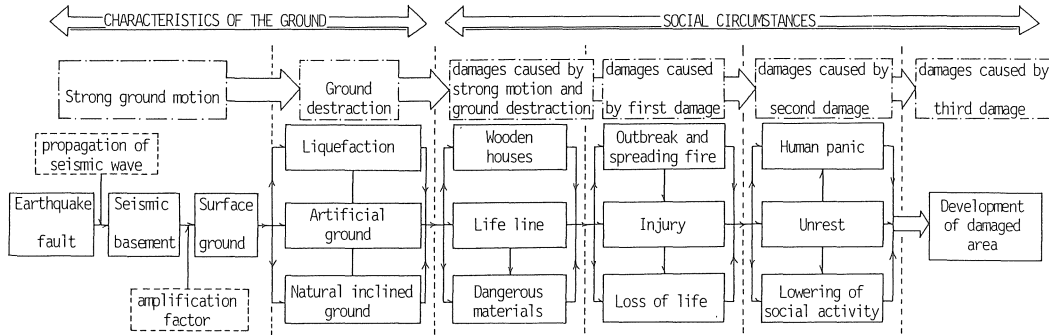


Figure 2 Detailed system of damage occurrence

This damage 1 acts again as the impact to regional circumstance which is changed by the damage 1, and damage 2 is produced. In the same manner as damage occurrence which was mentioned above, the earthquake damage m is finally produced to the regional circumstance, that is, presented social circumstances are changed by various damages from 1 to m.

Detailed system of the earthquake damage occurrence is shown in Figure 2, where various damages are related to each other and are in succession from the damage of ground destruction to the third damage. Namely, the damage of ground destruction such as liquefaction, artificial ground and natural inclined ground is generated by the strong ground motion on the surface. Furthermore first damage such as destroyed wooden houses, life line and dangerous materials is occurred corresponding to the degree of strong ground motion and ground destruction. The second damage caused by the first one is considered to occur the damage of outbreak and spreading fire, injury and loss of life. These damages occurrence as shown in the flow in Figure 2 are mainly based on experiences in the past. The detailed system of damage occurrence will be equivalent to the real damage system due to earthquake.

In this paper, the authors have discussed the items which are marked with shade in Figure 2, considering social circumstances, ground motion, ground destruction and earthquake damages in Nagoya city. Damage estimation was made in each meshed area, 500×500 m<sup>2</sup> in area, taking account of the ground structure and distributions of houses,

dangerous constructions and so on.

### 3. CALCULATION OF STRONG GROUND MOTION

#### (1) Estimation of Seismic Wave at the Ground Surface

It is well known that the spectrum of the earthquake ground motions observed on the surface can be represented as the product of the spectrum of the incident wave from the seismic basement and the amplification factor of the ground as follows ;

$$S_i(T) = O(T) \cdot P(T) \cdot G_i(T) \tag{1. a}$$

$$S_i'(T) = S_i(T) \cdot C_i(T) \tag{1. b}$$

where  $S_i(T)$  and  $S_i'(T)$  are the spectrum of the ground motion at the surface in an area  $i$ , and are considerably calculated in a case of flat soil layer such as plane area and of irregularity ground, respectively.  $O(T)$  is the initial spectrum from the earthquake fault.  $P(T)$  is the characteristics of the wave propagation from earthquake fault to the seismic basement.  $G_i(T)$  is the amplification factor of the ground,  $C_i(T)$  is the characteristics of the seismic amplification factor depending on the ground irregularity such as man-made ground and slope.

#### (2) Calculation of seismic motion on the basement<sup>0</sup>

Although there are many analytical methods of equation (1·a), we, at first, divided the right-hand side functions into the two functions,  $O(T) \cdot P(T)$  and  $G_i(T)$ .  $O(T) \cdot P(T)$  is calculated based on the estimation method of seismic wave spectrum using earthquake fault model. Basic assumption of the method is the fracture at the seismic fault starts at one point and

spreads step by step. If the fault plane is divided into (n) finite segments, each segment is considered the finite moving source. Then the observed seismic vibration is synthesized one of finite moving sources and its vibration amplitude is assumed to be synthesized amplitude of initial wave impulse from the finite sources. Initial wave impulse (Ii) from each source is given as follows;

$$I_i = \frac{d}{n \cdot (2 \cdot d's + d'x)} \cdot \log Sv_o (T) \quad (2)$$

where d is the duration time (sec) of seismic wave and is given by the following empirical equation;

$$d = 0.13 \times 10^{0.42M} + 0.24 \cdot X \quad (3)$$

X is the distance (km) from fault center to observed point and M is magnitude of earthquake. d's in equation (2) is the propagation time of fracture in source. d'x is the propagation time of radiated initial impulse from source and is given as follows;

$$d'x = 0.24 \cdot X_i \quad (4)$$

where Xi is the distance (km) from finite source to observed point. Log Sv<sub>o</sub> (T) is velocity response-spectrum of incident wave from seismic basement and is given experimentally as follows;

$$\log Sv_o (T) = a (T) \cdot M - b (T) \cdot \log X - c (T) \quad (5)$$

where X is the hypocenter distance, and a, b and c are parameters depending on the wave period (T) ranging from 0.1 to 5 seconds as shown in Figure 3. Response spectrum of incident wave on the seismic basement is obtained as an synthesized one of the initial impulses Ii from finite sources.

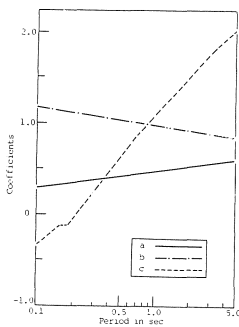


Figure 3 Coefficient a, b and c which are depending on periodic time

On the other hand, impact of earthquake damage is discussed generally on the bases of the maximum acceleration of ground motion. The acceleration spectrum of incident wave Sa (T) is a differentiation of Sv<sub>o</sub> (T). The maximum acceleration Amax is calculated from the following relation between Amax and

response spectrum attenuated 5% given by Kobayashi et. al.

$$A_{max} = 1.2 \times \text{M.S.I} \quad (6)$$

$$\text{M.S.I} = \int_{0.1}^{0.5} Sa (T) dT \quad (7)$$

where M. S. I is Modified Spectrum Intensity.

(3) Calculation of Strong motion on the ground surface

Gi (T) in equation (1 · a) has been studied by many authors such as Herrera and Rosenblueth, and is amplification characteristics of surface ground given by multiple reflection theory of SH wave.

For the calculation of Ci (T) in equation (1 · b), S-wave multiple reflection theory applied for the ground with flat layered structure can not be applied for the ground with irregular structure such as man-made ground and hill. One of our ground models with irregular surface is shown in Figure 4. In such a specific

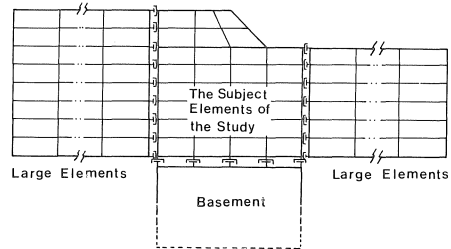
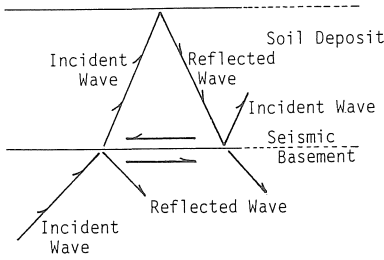


Figure 4 F.E.M model to the calculation of man-made ground and slope

ground, the finite element method (FEM) has been used commonly in engineering division. Therefore, we adopted the FEM to calculate Ci (T). There are, however, two problems when we use the FEM for response analysis of the ground with semi-infinite field. One of them is that if bottom boundary plane is assumed as a fixed plane, all the seismic energy entered from basement deposit in segmentally layer, and calculated seismic response in the system is evaluated larger than real response. Other one is that even though assumed wave discussed later enters vertically into the finite field from the underlying semi-infinite field, it produces horizontal propagation component of wave due to the irregularity of ground structure. This problem is to solve the condition of complete absorption of any wave at the lateral boundary plane.

As shown in Figure 4, the first problem is solved to carry out, at first, the response analysis in basement by S-wave multiple reflection theory and then to use the response results as input data to the ground to be analyzed. In this case, dispersion of seismic wave is to occur in the basement. The second problem is



**Figure 5** The viscoelastic system with vertical propagation of shear wave

solved by set-up of large elements, in the lateral side, which have enough size to absorb the reflected wave from the lateral boundary plane. The boundary condition mentioned above is made by the use of viscous boundary condition proposed by Lysmer. The stress condition of the FEM model system is shown in Figure 5. In the system, when function of displacement underlying finite field is represented as  $d(x, z)$ , the fundamental kinetic equation is given by

$$M \cdot \ddot{U} + K \cdot U = p \cdot \delta \quad (8)$$

where  $M$ : mass,  $K$ : stiffness constant,  $U$ : displacement.  $p$  is shear stress on the boundary plane.

On the other hand, displacement  $u$  on the seismic basement is,

$$u = f(t - z/v) + g(t + z/v) \quad (9)$$

based on the theory of elasticity, where,  $f$ : incident wave,  $g$ : reflective wave and  $v$ : S-wave velocity. Shear stress,  $s$ , is calculated by differentiating equation (9),

$$s = r \cdot v \cdot (\dot{u} - 2 \cdot \dot{f}) \quad (10)$$

when equation (8) is rearranged by substituting equation (10) into

$$M \cdot \ddot{U} + K \cdot U = -d\delta \cdot \dot{u} + d\delta \cdot 2\dot{f} \quad (11)$$

where,  $r$  and  $d\delta$  are the density and  $d\delta = \delta \int r \cdot v \cdot dz$ , respectively. And then, discretizing the equation (11), we get the fundamental kinetic equation for FEM.

$U$  and  $U_0$  are the displacement of subject elements and of large elements in the lateral side, respectively, under the condition that the displacement of the boundary plane is continuously. As the displacement at the lateral boundary plane is continuous from lateral side to the subject area, displacement,  $U$ , in subject area is given at the boundary plane as

$$U = U_0 + \varphi \quad (12)$$

where  $U_0$  is the displacement in the lateral large element and  $\varphi$  is the displacement in the lateral area displacement produced by inhomogeneity. Shear stress,

$s$ , in the subject area is calculated by,

$$s = r \cdot v \cdot \dot{u} = r \cdot v \cdot (\dot{u}_0 + \dot{\varphi}) \quad (13)$$

This equation is rearranged based on the boundary condition into

$$s = r \cdot v \cdot \dot{\varphi} = r \cdot v \cdot (\dot{u} - \dot{u}_0) \quad (14)$$

combining equation (14) and (8),

$$M \cdot \ddot{U} + K \cdot U + r \cdot v \cdot A \cdot \dot{u} = r \cdot v \cdot A \cdot \dot{u}_0 \quad (15)$$

where  $A$  is an area of boundary plane. Solving the equation (11) and (15), we can obtain the vibration characteristics at the irregular ground such as Figure 4.

Finally, seismic vibration spectrum in equation (1) is calculated by using of equation (2) for  $O(T) \cdot P(T)$  and Herrea and Rosenbluth's method for  $G_i(T)$  and equation (15) for  $C(T)$ , and then it is calculated that the maximum acceleration is obtained by using the seismic vibration spectrum at ground surface in each meshed area.

#### 4. METHOD OF DAMAGE ESTIMATION TO WOODEN HOUSE

Recent investigations on earthquake damage have been suggested that damages of wooden houses are due to two main factors, i.e, strong ground motion and destruction of ground such as liquefaction and land slide. Therefore, in this paper, earthquake damages of wooden houses,  $P_t$ , are represented as follows;

$$P_t = \{p_1(a) \text{ or } p_2(l)\} + p_3(m) \quad (16)$$

where  $p_1(a)$ ,  $p_2(l)$  and  $p_3(m)$  are totally destroyed ratio depending on the maximum ground acceleration, liquefaction and man-made ground destruction, respectively.

##### (1) Damage caused by the strong ground motion

Damage due to  $p_1(a)$  is referred from the correlation between acceleration on the ground surface and the totally destroyed ratio proposed by Mononobe<sup>2)</sup> and Kagami.<sup>3)</sup> Their relation is shown in Figure 6, where the broken line and the solid circles are the result between the maximum acceleration and totally destroyed ratio by Mononobe and Kagami, respectively. Their data are of earthquake damage before 1950. Considering that most of the recent wooden houses are more resistant to seismic vibration than the past ones. Hence, we accepted solid curve as  $p_1(a)$  estimation. This defined curve is about 0.75 times to Mononobe's one.

##### (2) Damage caused by liquefaction

Damage to wooden houses caused by liquefaction,  $P_2(l)$ , is estimated from the relation between the

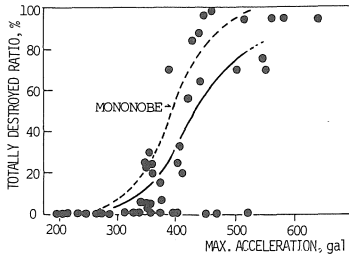


**Figure 6** Relation between the maximum acceleration on the ground and totally destroyed ratio of wooden houses

degree of liquefaction and totally destroyed ratio. The degree of liquefaction is estimated by Iwasaki's method<sup>4)</sup> which gives the numerical values as a degree of liquefaction. The outline of this method is summarized as follows.

Maximum shear stress,  $S_{max}$ , in each depth is shown as

$$S_{max} = (A_{max}/g) \cdot V_v \cdot (1.0 - 0.015 \cdot Z) \quad (17)$$

where  $A_{max}$ ; maximum acceleration at the ground surface,  $g$ : gravity,  $V_v$ : normal stress,  $Z$ : depth in meter.

On the other hand, the resistivity of soil,  $R$ , is

$$R = C \cdot R_e \quad (18)$$

where  $C$  is the correction factor depending on the irregularity of seismic wave, the density of soil, etc.  $C$  is assumed as 0.95.  $R_e$  is calculated by empirical equation and is given as;

$$R_e = R_f - 0.22 \cdot \log \cdot (D_{50}/0.35) \quad (19)$$

$(0.04 \leq D_{50} < 0.6)$

$$R_e = R_f - 0.55 \quad (0.6 \leq D_{50} \leq 1.5) \quad (20)$$

where  $D_{50}$  is the diameter (mm) of sandy soil at 50 percents of the particlesize accumulation curve, and  $R_f$ :  $R_f = 0.088 \cdot Z \cdot (N/V_v' + 0.7)^{1/2}$ ,  $V_v'$ : effective pressure.  $N$  is standard penetration value. The safety factor,  $FL$ , to liquefaction in each depth is defined as;

$$FL = R/S_{max} \quad (21)$$

and based on the variation of  $FL$  to the depth, the degree of liquefaction,  $PL$ , is

$$PL = \int_0^{20} F \cdot W(z) \cdot dz \quad (22)$$

where  $F = 1.0 - FL$  when  $FL$  is smaller than 1.0 and  $F = 0.0$  at  $FL$  value more than 1.0.  $W(z)$  is assumed as  $W(z) = 10.0 - 0.05 \cdot Z$ . Referring the data of the past earthquake damage (Nobi, Tonankai and Mikawa Earthquake), we calculated the totally destroyed ratio and the  $PL$  value by means of the equation (22) at the liquefaction area, and the relation of both

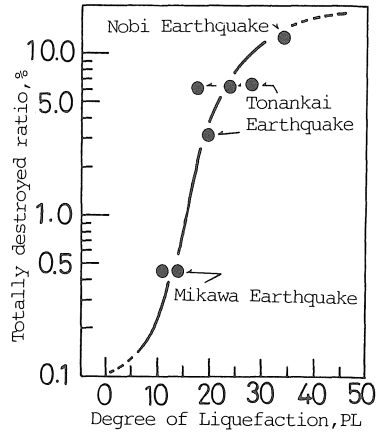


**Figure 7** Relation between the degree of liquefaction and totally destroyed ratio

was shown in Figure 7.

The totally destroyed ratio rapidly increase in the range of  $PL = 10 - 15$ . From this patterns, we accepted the solid curve, Vulnerability Function, in Figure 7, for  $P_2$  ( $I$ ) estimation from the totally destroyed houses.

*(3) Damage on the man-made ground*

As an estimation of  $P_3$  ( $m$ ) damage, we study the relation between maximum acceleration on the man-made ground and totally destroyed ratio based on detail analyses of The Midorigaoka man-made grounds damaged during the Miyagiken-oki Earthquake ( $M = 7.8$ ) in 1978. Figure 8 shows the geological maps and crosssection of ground before and after construction of the Midorigaoka ground.

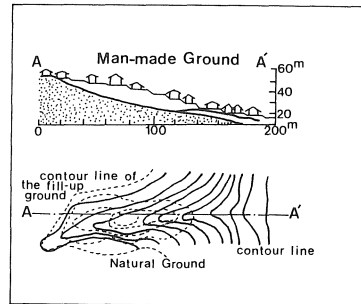


**Figure 8** Geological map at Midorigaoka man-made ground

Damage of houses on the man-made grounds during the earthquake are mainly considered to be caused by the destruction of the man-made grounds. Asada investigated the relation between the geological condition of man-made grounds and damages of houses, and reported that seismic damage was scarce in cut-off ground but it occurred mostly in fill-

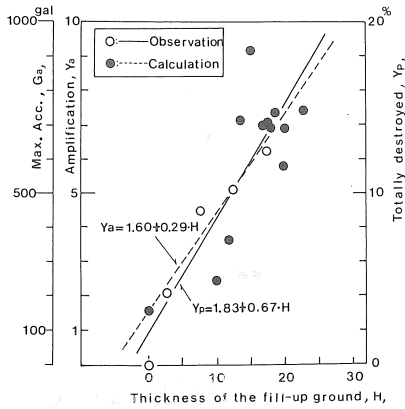


**Figure 9** Relation among the thickness of the fill-up layer, totally destroyed ratio and the estimated maximum acceleration of the man-made ground in the Miyagiken-oki Earthquake (1978)

up ground and it did remarkably in the fill-up ground developed around stream basin. Based on his report, the relation between thickness of fill-up ground and totally destroyed ratio is obtained on the case of Midorigaoka, Sendai city. The result has shown in Figure 9. It is that totally destroyed ratio of houses are directly proportional to the thickness of the fill-up layer which lies on the sandstone layer. This relation obtained from the least square method is given as follows;

$$Y_p = 1.83 + 0.67 \cdot H \quad (23)$$

where  $Y_p$  is totally destroyed ratio and  $H$  is the thickness of fill-up ground. The cross section, A-A', of the Midorigaoka ground in Figure 8 was used for preparing the model ground shown in Figure 10. Density and S-wave velocity of ground, which are necessary for the calculation, are estimated from N-value by the following empirical equations (Iida, et. al, 1978)

$$V_s = 103.62 \cdot N^{0.312}$$

$$R_o = 1.635 \cdot N^{0.044}$$

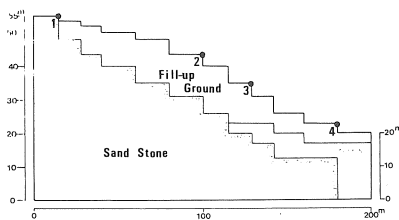


**Figure 10** The calculation model of the man-made ground in Midorigaoka

Although most of the N-value for the equations are from Asada's investigation, in cases of debris and sandstone without N-value data, S-wave velocity and density are assumed as 250m/s and 1.80 in the debris and 1200m/s and 2.30 in the sandstone, respectively.

Figure 11 shows parts of results of seismic response analysis calculated from the physical parameters mentioned above. They are corresponding to the response spectrum at site 1 to 4 in Figure 10.

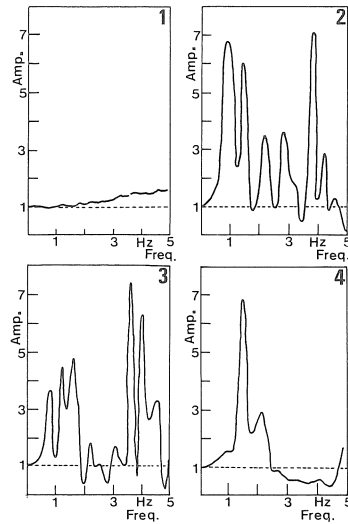


**Figure 11** Characteristics of the response spectrum on the site 1 to 4 in the F.E.M model as shown in Figure 10.

As the site 1 consists of sandstone layer, amplification factor obtained is about 1 in all frequency range. On the other hand, the site 2 and 3 have spectrum structures with two peaks around 1.0 Hz and 3.8 Hz, and amplification factor in the site 2 and 3 are about 7 and about 3.8 around 1 Hz, respectively. The site 4 has a peak around 1.3 Hz and its amplification factor is about 6.8. If we assume that upper of sandstone is fill-up ground, we can find tendency of the amplitude increasing with thickness of the ground. However, peak frequencies show no systematic relation with the thickness, but are usually around 1.0 Hz and 3.8 Hz. From these results, it is clear that amplitude is directly related to the thickness of fill-up ground. From the relation between amplification and damage conditions in Figure 9, this relation between the amplification factor,  $Y_a$ , and the thickness of fill-up layer is given as follows;

$$Y_a = 1.60 + 0.29 \cdot H \quad (24)$$

On the other hand, calculated maximum acceleration of the basement<sup>5)</sup> around Sendai city, 20 km north from the Midorigaoka man-made ground, is

about 100 gals. If we assumed that incident wave passing through basement has maximum acceleration of 100 gals, the maximum acceleration at the surface on the man-made ground,  $G_a$ , is calculated as follows;

$$G_a = 100 \cdot Y_a \tag{25}$$

From the equations (23), (24) and (25), the relation between maximum acceleration on the man-made ground and totally destroyed ratio is re-written as follows;

$$Y_p = -1.87 + 0.0033 \cdot G_a \tag{26}$$

However, the empirical equation (26) can be applied to the case of the maximum acceleration more than 230 gals at the surface, because the damages occurred at the ground with the more than this value.

After we apply the damage estimations mentioned above to each meshed area and synthesize all the damage, we evaluated the total damage in each meshed area.

**5. ESTIMATION METHOD OF FIRE DAMAGE**

Fire damage caused by earthquake depends on the number of outbreak fire and their spreading. It is necessary that number of outbreak fire and its location are estimated. Hence, outbreak fire ratio,  $Y_i$ , in any area,  $i$ , is assumed as;

$$Y_i = f(X_{1i}, X_{2i}) \tag{27}$$

where  $Y_i = y_i/N_i$ ,  $y_i$  is the number of outbreak fire,  $N_i$  is the total number of wooden houses,  $X_{1i}$  and  $X_{2i}$  are outbreak fire ratio depending on the totally destroyed ratio, and on the number of dangerous materials such as boilers, dangerous chemicals, factories and restaurants, respectively.

The relation between  $Y_i$  and  $X_{1i}$  is obtained by using the data of earthquakes damages after 1872.

As shown in Figure 11,  $Y_{i1}$  is related to  $X_{1i}$  by the following equation (28).

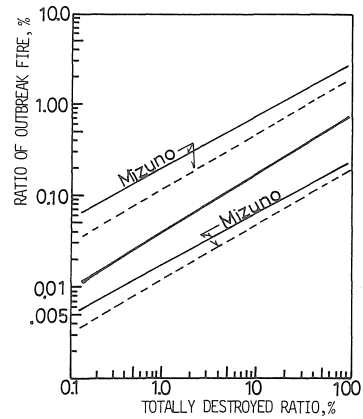


**Figure 12** Relation between the totally destroyed ratio and the outbreak fire ratio

$$\log Y_{i1} = 0.648 \cdot \log X_{1i} - 1.417 \tag{28}$$

On the other hand, in a general sense, the ratio of outbreak fire ( $X_{2i}$ ) which depends on the dangerous materials increases in proportion to their number ones. They are classified into three types based on their characteristics such as factories, dangerous chemicals and restaurants. The three types of dangerous articles are divided into five classes according to their number in  $500 \times 500 \text{ m}^2$  mesh area. We defined the index of the outbreak fire risk ( $df_{i,j}$ ) from 0 to 5 which are depending number of dangerous materials as shown in Table 1, and then the relation between the outbreak fire ratio ( $X_{2i}$ ) and total number of its risk index ( $\sum_{j=1}^3 df_{i,j}$ ) which is added up to three types of dangerous articles in each mesh area as following equation.

$$X_{2i} = 0.033 \cdot \sum_{j=1}^3 df_{i,j} \tag{29}$$

A number of outbreak fire in each mesh area is obtained from the number of houses multiplied by the outbreak ratio ( $Y_i$ ) using the equation (28) and (29).

**Table 1** Index of the outbreak fire risk according to the number of dangerous materials

dangerous materials	index of the outbreak risk ( $d_i$ )					
	0	1	2	3	4	5
factory	0	1-9	10-29	30-49	50-69	70-
dangerous chemical	0	1-4	5-9	10-14	15-19	20-
restaurant	0-9	10-49	50-99	100-149	150-199	200-

At second step, we make a description of the estimation of the damage to the spreading fire. Damage caused by spreading fire is estimated from complex

social circumstances around the outbreak site and weather conditions. We studied the big fire damage on the past twenty big fires to discover the major factors

which cause fire spreading. Consequently, authors found that wind velocity, mixed ratio of wooden house and space distance between the houses increased fire spreading, whereas open space, river, park, fire-proof buildings and fire-prevention facilities work against the fire spreading. Authors will estimate the fire damage using only, the former spreading fire factors. Subsequently the damage is re-evaluated by the latter reduction factors of fire-spreading velocity equation, we used Horiuchi's equation as following.

$$Ki_{i=1,3} = (a/2+d) + (x-T) \cdot (a+d)/Ti_{i=1,3} \quad (30)$$

Provided that, when T is more than x,

$$Ki_{i=1,3} = (a/2+d) \cdot x/T.$$

where  $Ki_{i=1,3}$  is the fire spreading distance after x minutes in each area.  $i=1$  to 3 is the wind direction to the leeward, windward and their cross section, respectively. a is length of the wooden house in meter, and d (meter) is the distance of pitch from house to house.  $Ti_{i=1,3}$  is the fire-spreading time (minute) as follows ;

$$Ti_{i=1,3} = (ti_{i=1,3} \cdot 0.01 \cdot f) + (ui_{i=1,3} \cdot 0.01 \cdot q) \quad (31)$$

where  $ti_{i=1,3}$  and  $ui_{i=1,3}$  are the time which is required for the caught fire from house to house concerning about wooden and fire-retardant wooden house, respectively. f and q are mixing ratio of wooden house for general and fire-retardant wooden house, respectively. If we set the infinite time into equation (30), the calculated spreading distance is also infinite. However, in generally, the fire spreading area stopped in any site when even in an earthquake. This phenomenon is considered about two factors which consist of both the artificial and the natural factor. The former factor is the artificial prevention power which is depending on the activity of fire fighting power, the latter one is the natural circumstance such as open space, river, park and fire-proof building. Therefore, in this study, two factors mentioned above are considered in the formula of spreading velocity of fire.

At first, the artificial prevention power by the activity of fire fighting will be dropped by the damage of water supply and by the traffic panic. Subsequently, as shown in Figure 13, this factor is assumed that correction value, c, has the effect of the reduction of the fire-spreading velocity but does not have the effect of the stop of the fire-spreading. Using this correction value, the equation (31) is re-expressed as follows ;

$$Ti_{i=1,3} = \{(ti_{i=1,3} \cdot 0.01 \cdot f) + (ui_{i=1,3} \cdot 0.01 \cdot q)\}/C \quad (32)$$

where the correction value of the fire spreading depends on water content in fire prevention pool of earthquake-proof.

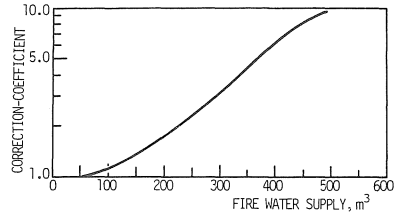


Figure 13 The correction coefficient to the quantity of fire water supply

At second, we assumed that natural prevention factor is based on the data of big fire experimentation, and the effect on this factor is decided that fire-spreading is stopped at open space, river and fire-proof building, each width of which being more than 20 meters.

### 6. ESTIMATION OF LOSS OF LIFE

The loss of life is estimated with the number of totally destroyed houses obtained using the data of earthquakes damages after 1872 in Japan. As shown in Figure 14, the relation between number of totally destroyed houses and number of loss of life is not monotonical function, but the slope of the curve tends to change at the value whose the number of totally destroyed house is 500. Hence, two slopes are determined by fitting data into the method of linear least squares. The equations of solid lines in Figure 14 are written as follows ;

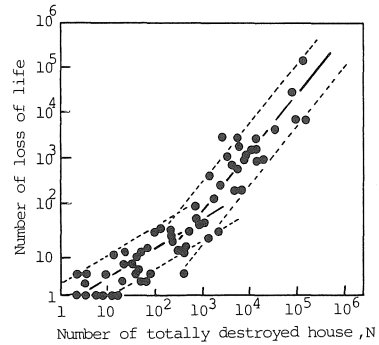


Figure 14 Relation between the number of totally destroyed houses and the number of loss of lives

$$\text{Log } D = 1.23 \cdot \text{log } N - 1.84 \quad (N > 500) \quad (33)$$

$$\text{Log } D = 0.64 \cdot \text{log } N - 0.24 \quad (1 < N \leq 500) \quad (34)$$

where D is the number of loss of life and N is the number of totally destroyed houses.



## 7. DECISION OF COMPREHENSIVE SEISMIC RISK

For the possibility of the seismic risk in any site, seismic risk assessment is obtained under the consideration of the various earthquake damage, because the earthquake damage consists of the damages from the multifarious sources. In this study, the comprehensive seismic risk is defined by the addition of the various earthquake damage. The comprehensive seismic risk,  $S_r$ , is shown as follows;

$$S_r = \sum_{i=1}^n K_i \cdot R_i \quad (35)$$

where  $K_i$  is the weighting factor which has the value of 1 or 2.  $R_i$ , with the range between 0 to 7, is the damage rank which is defined by dependence on the degree of damages. In Nagoya city, authors will estimate the comprehensive seismic risk assessment in each mesh area in the paper of part 2.

### ACKNOWLEDGMENT

The authors would like to Dr. Kazuaki Masaki of Aichi Institute of Technology for his useful discussions, and express gratitude to the staffes for the Earthquake Prevention Committee of Nagoya City.

## REFERENCES

1. S. Midorikawa and H. Kobayashi ; On Estimation of Strong Earthquake Motions with Regard to Fault Rupture, Trans. of A.I.J, No.282, August, 1979 (in Japanese with English abstract)
2. N. Mononobe ; DOBOKU TAISHINGAKU, Tokiwa Books, 1938 (in Japanese)
3. H. Kagami and H. Kobayashi ; Intensity of Ground Motions During the Kanto Earthquake 1923 in Kawasaki (Subsoil Conditions and Damage Ratio of Wooden Houses due to Earthquake), Trans. of A.I.J, No.176, Oct. 1970 (in Japanese with English abstract)
4. T. Iwasaki, F. Tatsuoka, K. Tokita and S. Yasuda ; Estimation of Degree of Soil Liquefaction During Earthquake, J.S.S.M.F.E, Vol.28, No.4, 1980 (in Japanese)
5. T. Kunii ; On the Maximum Acceleration Estimated from Investigation of Tombstones Comprehensive Urban Studies, No.8, 1979. (in Japanese with English abstract)
6. H. Taniguchi, K. Masaki, T. Tsuboi and K. Iida ; Damage to Ground Structures and Grave Stones Caused by the 1978 off Miyagi Earthquake, Bull. Aichi. Ins. Tech, Vol.14, 1979 (in Japanese)

(Received January 25. 1986)